Available online at www.sciencedirect.com
SCIENCE DIRECT
Talanta 68 (2005) 131–137
Talanta
www.elsevier.com/locate/talanta

Electrochemical impedance probing of DNA hybridisation on oligonucleotide-functionalised polypyrrole

Chaker Tlili [a,b], Hafsa Korri-Youssoufi [b], Laurence Ponsonnet [a], Claude Martelet [a], Nicole J. Jaffrezic-Renault [a,*]

[a] *Cegely, UMR-CNRS 5005, EC-Lyon, 69134 Ecully Cedex, France*
[b] *Laboratoire de Chimie Bioorganique et Bioinorganique UMR-CNRS 8124, Institut de Chimie Moléculaire et Matériaux d'Orsay, Université Paris-Sud, 91405 Orsay, France*

Received 7 January 2005; received in revised form 4 April 2005; accepted 27 April 2005
Available online 9 June 2005

Abstract

We report a new approach for detecting DNA hybridisation using non faradaic electrochemical impedance spectroscopy. The technique was applied to a system of DNA probes bearing amine groups that are immobilized by covalent grafting on a supporting polypyrrole matrix functionalised with activated ester groups.

The kinetics of the attachment of the ss-DNA probe was monitored using the temporal evolution of the open circuit potential (OCP). This measurement allows the determination of the time necessary for the chemical reaction of ss-DNA probe into the polypyrrole backbone.

The hybridisation reactions with the DNA complementary target and non complementary target were investigated by non faradaic electrochemical impedance spectroscopy. Results show a significant modification in the Nyquist plot upon addition of the complementary target whereas, in presence of the non complementary target, the Nyquist plot is not modified. The spectra, in the form of Nyquist plot, were analysed with the Randles circuit. The transfer charge resistance R_2 shows a linear variation versus the complementary target concentration. Sensitivity and detection limit (0.2 nM) were determined and detection limit was lower of one order of magnitude than that obtained with the same system and measuring variation of the oxidation current at constant potential.

Keywords: Label-free detection; DNA hybridisation; Equivalent circuit; Charge transfer resistance

1. Introduction

The development of DNA-based biosensors will provide a powerful new technique for rapid detection of pathogens, human genetic disorders, routine health assessment of water and food quality, and for screening of drugs that may bind to DNA or regulate gene expression. Consequently, they offer the possibility of performing reliable diagnosis before any symptoms of a disease appears [1–4].

In the past few years, there has been interest in developing alternative technologies to monitor hybridisation with a high selectivity. Biosensors based on surface plasmon resonance [5,6], optical fibre [7], quartz crystal microbalance [8], and microcantilever [9] are the four main approaches. A particularly interesting method is obtained by combining the specificity of hybridisation with the analytical power of electrochemical methods [10–13]. Most of the optical and electrochemical methods are indirect and need a labelling of target-DNA with fluorescent dyes, redox indicators or metal complex. A great advantage of electrochemical biosensors compared to the other types of biosensors is that they can be integrated in small, inexpensive devices offering high sensitivity, low cost, fast detection [14]. Impedance spectroscopy is an effective tool to probe the interfacial properties (capacitance, electron-transfer ability) of modified

* Corresponding author. Tel.: +33 472186243; fax: +33 478433717.
E-mail address: Nicole.Jaffrezic@ec-lyon.fr (N.J. Jaffrezic-Renault).

0039-9140/$ – see front matter © 2005 Elsevier B.V. All rights reserved.
doi:10.1016/j.talanta.2005.04.069

electrodes and it can be used to probe DNA hybridisation and serve as a basis for innovative DNA biosensors or arrays [15–19].

The immobilization step of the DNA probe into the surface plays a major role in determining the overall performance of an electrochemical DNA biosensor. The achievement of high sensitivity and selectivity requires minimisation of non-specific adsorption and the stability of immobilisation. Control of the surface chemistry and coverage is essential in order to ensure high reactivity, orientation, accessibility and stability of the surface confined probe. A common way for immobilization of receptors on the surface in the construction of the biosensor devices is the use of surface assembled monolayers (SAM). The SAM is previously substituted by carboxy groups, which can link an amino group of the biological probe to form a peptide bond. This coupling reaction is mediated by a carbodiimide EDC [20], often used together with *N*-hydroxysulfosuccinimide (NHS) [21]. Another possibility is to use the high stability of streptavidin/biotin interaction, by the immobilisation of biotinylated DNA oligomers at the SAM modified with streptavidin [22]. Another very direct technique is to modify the DNA oligomer by a thiol linker which can be used for direct binding to the metal surface in order to form SAM. Despite the attractive nature of these approaches, the immobilisation of a DNA probe using SAM techniques cannot form densely packed layers. This is due to the large hydrophilic nucleic acid group and therefore the stability of the layer is questionable, especially at high temperatures [23].

Conducting polymers make a highly suitable interface for grafting DNA probes onto a micro-sized surface [24]. This is due to their easy processability into thin films onto conducting electrodes combined with their large surface area and their ability to convey the biological recognition process into a useful analytical signal. The most commonly used conducting electroactive polymer (CEP) in sensing applications is polypyrrole (PPy) owing to its biocompatibility, high hydrophilic character combined with high stability in water and facile incorporation of many counter ions [25]. The immobilization of DNA on electrodes modified with conducting polypyrrole has been previously accomplished using three approaches. The first approach involves a direct adsorption of ssDNA onto oxidized PPy films [26]. In this case, the delocalized positive charge of the oxidized polymer electrostatically attracts the negatively charged phosphate group of DNA. The second approach involves incorporation of oligonucleotides into the polymer matrix during the growth of the conducting polymer [27–29]. The third approach involves the development of a precursor polymer bearing an easy leaving ester group on which amino-labeled oligonucleotides were directly substituted [30–33]. In this case, polypyrrole substituted by ss-DNA probes demonstrated good sensitivity and selectivity to the ss-DNA target using cyclic voltammetry however the electrical properties of polypyrrole after such reaction was not characterized. In this work, the kinetics of this reaction was studied using open circuit potential (OCP) methods, then the electrical properties of the PPy-DNA film were studied by impedance spectroscopy, which tracked both the grafting of the ss-DNA probe and the direct hybridization of ssDNA complementary target and non complementary target. With the aid of an electrical equivalent circuit designed to represent the aforementioned system, various parameters of the PPy-DNA films were deduced such as capacitance and charge transfer resistance during the hybridisation reaction.

2. Materials and methods

2.1. Reagents

The 3-*N*-hydroxyphthalimide (**I**) and 3-acetic acid pyrrole (**II**) were synthesized as described previously [34]. The oligonucleotide probe ss-DNA is 25-mer bear a terminal amino group on its 5′ phosphorylated position with the sequence: NH_2-5′-TCA-ATC-TCG-GGA-ATC-TCA-ATG-TTA-G-3′. Oligonucleotide targets, complementary to the oligonucleotide probe were 25-mer with the sequence 5′-CTA-ACA-TTG-AGA-TTC-CCG-AGA-TTG-A-3′, the non complementary target is 24-mer with sequence 5′-TAA-AGC-CCA-GTA-AAG-TCC-CCC-ACC-3′. Stock solutions of the target and non-complementary oligonucleotides with various concentrations were prepared in a 10 mM phosphate buffer solution and stored in a freezer until use.

2.2. Electrochemical polymerisation

Electrochemical polymerization and characterization were performed in a one-compartment three electrode cell with gold as working electrode. The solution was de-gassed by bubbling argon. The precursor copolymer (Scheme 1), poly [3-acetic acid pyrrole, 3-*N*-hydroxyphthalimide pyrrole)] (**III**) was electropolymerized in acetonitrile containing the monomers 3-acetic acid pyrrole (0.06 M) and 3-*N*-hydroxyphthalimide pyrrole (0.04 M) at a fixed potential of 1 V versus Ag/AgCl during 15 s. The concentration of the monomers was chosen in order to obtain the highest electroactivity in aqueous media.

2.3. Covalent grafting of ss-DNA probes onto polypyrrole

A direct chemical substitution of the leaving group *N*-hydroxyphthalimide by the oligonucleotide was obtained by soaking the supported film of PPy into a solution of the oligonucleotide probe bearing a terminal amino group on its 5′ phosphorylated position. This reaction was carried out for 3 h in 5 ml of 0.1 M $LiClO_4$ solution of acetonitrile (ACN) containing 10% phosphate buffer at pH 6.8 and 25 nmoles of the ss-DNA probe. The electrode was carefully washed with water in order to remove any trace of ungrafted ODN probe.

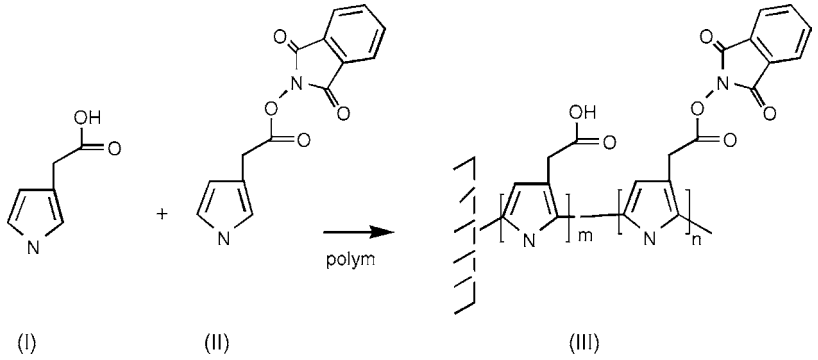

Scheme 1. Copolymerization reaction of the pyrrole bearing acid group and pyrrole bearing activated ester groups.

2.4. Hybridisation of ADN-polypyrrole with ss-DNA targets

Hybridization was performed at 37 °C by incubating the modified electrode in 10 mM phosphate buffer containing 137 mM NaCl and 2.7 mM KCl, at pH 7 in the presence of ss-DNA complementary target and non complementary target.

2.5. Impedance measurements

Non faradaic AC impedance spectroscopy and OCP measurements were obtained in a conventional three-electrode electrochemical cell with a Solartron 1287 Electrochemical Interface and a Solartron 1255B Frequency Response Analyser (Solartron Inc., U.K.). The different electrodes used were: a modified gold working electrode (0.12 cm^2 geometrical surface area), a Pt plate (0.64 cm^2 geometrical area) as counter electrode and a saturated calomel electrode (SCE) as a reference electrode. Impedance measurements were performed in 10 mM phosphate buffer (containing 137 mM NaCl and 2.7 mM KCl, pH 7).

The impedance measurements were performed, without any redox species, in the frequency range of 0.5–10^5 Hz with a sinusoidal potential in which modulation of ±10 mV amplitude was superimposed on a dc potential of −1400 mV. This highly negative potential was choosen in order to minimize Warburg impedance and to emphasize the contribution of the impedane of the PPy-DNA/electrolyte interface. At this potential, polypyrrole was at a non-doped and semiconducting state and no parasite electrochemical reaction occurred as measurements were performed under argon flow. Five points, equally spaced on a logarithmic scale, were acquired per decade increment in frequency. The impedance data were fitted with an electrical equivalent circuit using the Zplot/Zview software (Scribner Associates Inc.). The equivalent circuit provides an electrical analogue of chemical/physical processes.

In all impedance spectra presented here, symbols represent the experimental raw data, and the solid lines are the fitting curves obtained from equivalent circuits. The Nyquist plot was used to visualize the raw data and to evaluate the quality of data fitting over the entire frequency domain probed.

3. Results and discussion

3.1. Functionalisation of pyrrole by ss-DNA probe

The amino-substituted oligonucleotide, ssDNA, was grafted on the copolymer by a direct chemical substitution of the easy leaving group, *N*-hydroxyphtalimide (Scheme 2). The covalent grafting of ss-DNA to the copolypyrrole was confirmed using FT-IR spectroscopy by the formation of amide band formed between polypyrrole and ss-DNA after chemical reaction and disappearance of the frequencies associated with pyrrolidinedione. The time necessary for the complete reaction is less than three hours [11].

OCP monitored the immobilisation of the oligonucleotide and Fig. 1 presents the OCP curve for PPy coated on a gold electrode that was treated with 25 nmoles of ss-DNA probe. Upon injection, the potential shifts from 162 to −2 mV followed by progressive increase of the potential to stationary

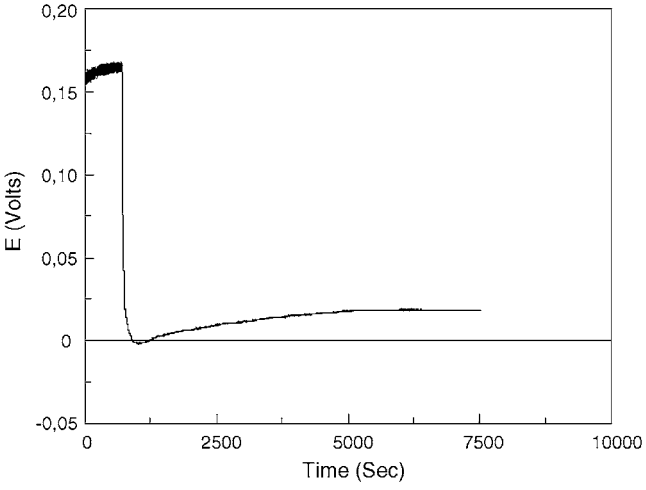

Fig. 1. Change in the open circuit potential of PPy/gold electrode after introduction of 25 nmol of ssDNA probe into an 5 ml acetonitrile solution of 0.1 M $LiClO_4$ and 0.5 ml of PBS solution at pH 7.

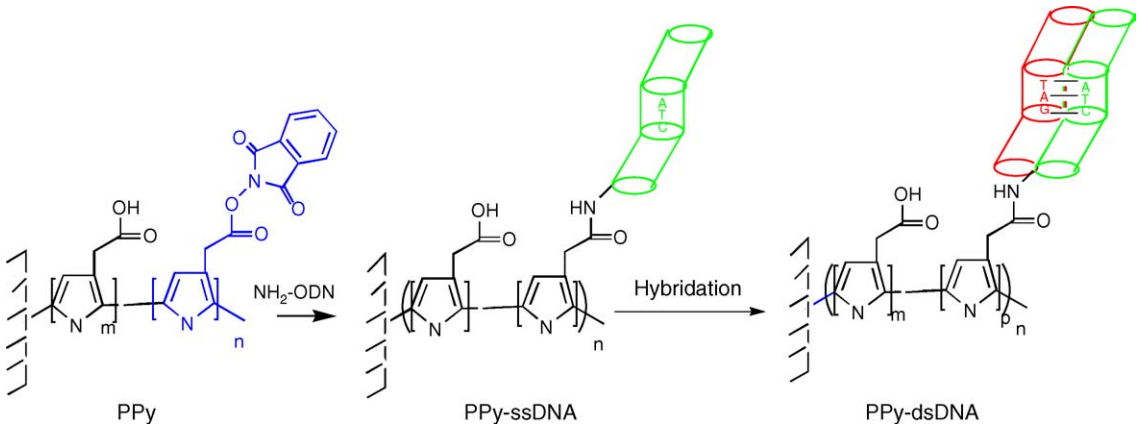

Scheme 2. Reaction of the grafted of ss-DNA probe into polypyrrole followed by hybridization of ss-DNA target.

value of 2 mV after 2 h of reaction. Intuitively, the variation of the OCP results from change in the accumulated charge on the electrode. A shift to more negative value is therefore indicative of an increase of negative charge at the surface of the copolymer coming from the anionic charge of phosphate present on the ss-DNA probe. As the polypyrrole is in the oxidative state at OCP and presents a cationic site [35], strong interaction occurred at the surface after addition of the ssDNA probe, which explains the negative shift in the OCP. This potential then increases and remains constant after 5000 s corresponding to a time necessary for the complete chemical reaction between amino-labeled DNA and easy leaving groups in the copolymer. Thus, the change of the OCP value observed in Fig. 1 is indicative of a two-step process. The first is an accumulation of negative charge coming from the ss-DNA to the polymer surface, and the second is a gradual discharge of this charge towards the bulk of the polymer by chemical reaction.

3.2. Characterisation of the grafted ss-DNA probe and hybridization of ss-DNA target by impedance measurements

Fig. 2 presents the Nyquist diagram of the copolypyrrole films on gold electrode obtained after polymerisation reaction and grafting of the ssDNA probe (Fig. 2), measured in the same experimental conditions. These results show a large modification of the Nyquist diagram after the grafting of ss-DNA on the copolymer film. The resistance of the charge transfer (electronic and ionic) decreases from 175.9 Ω cm^2 for PPy film to 63.9 Ω cm^2 for PPy-ssDNA. These values were obtained by fitting the experimental results with an equivalent circuit described in the next paragraph.

The modified PPy-ssDNA electrode was incubated for 1 h 30 min in PBS solution containing complementary ss-DNA target, and the impedance measurements are shown in Fig. 3. With complementary ss-DNA hybridisation takes place with the probe immobilized on the polypyrrole, producing an obvious enlargement of the Nyquist diagram (see

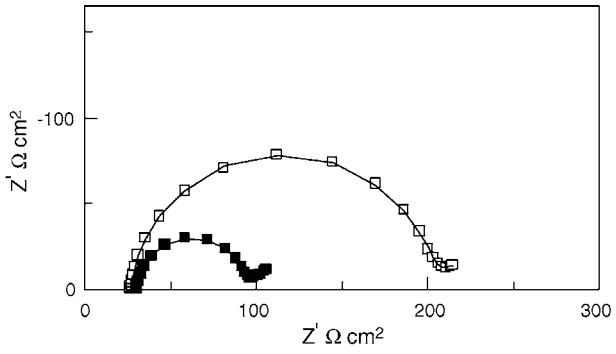

Fig. 2. Nyquist plots of PPy films prepared at the bare gold (□) before and after grafted of ss-DNA probe (■). Spectra were acquired at –1400 mV vs. (SCE) in PBS electrolyte, pH 7. The symbols are the experimental data, and the solid lines are results from the fitting data.

Fig. 3b–e). However, with non complementary ss-DNA target, the impedance measurements (Fig. 4) show a very small variation in the Nyquist plot. The impedance data obtained after hybridisation with target DNA, has been analysed with the Randles circuit [36] shown in Scheme 3, which gives an

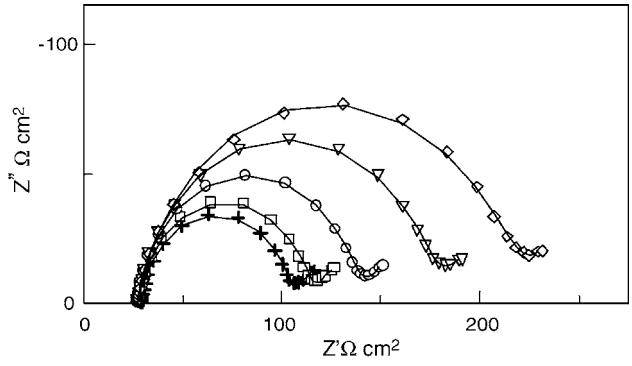

Fig. 3. Nyquist plot of a the PPy-DNA films after hybridization reaction with its complementary target under various concentrations: 0 nmol ml^{-1} (+); 0.5 nmol ml^{-1} (□); 2 nmol ml^{-1} (◯); 3.5 nmol ml^{-1} (▽) and 5.5 nmol ml^{-1} (◊). Impedance spectra were acquired at −1400 mV vs. (SCE) in PBS electrolyte, pH 7. The symbols are the experimental data, and the solid lines are results from the fitting data.

Table 1
Calculated value of Q_1, R_2 and Q_2 obtained from Randles equivalent circuit

DNA target (nmol ml^{-1})	Q_1		R_2 (Ω cm^2)	Q_2		χ^2 (10^{-4})
	Y_Q ($\mu\Omega^{-1}$ cm^{-2} s^n)	n		Y_Q ($\mu\Omega^{-1}$ cm^{-2} s^n)	n	
0	23.41	0.933	74.5	0.032	0.499	3.8
0.5	21.50	0.936	84.9	0.029	0.494	2.3
2	24.08	0.921	110.3	0.028	0.496	0.9
3.5	30.85	0.891	148	0.026	0.471	1.2
5.5	39.05	0.862	188.7	0.024	0.478	4.1

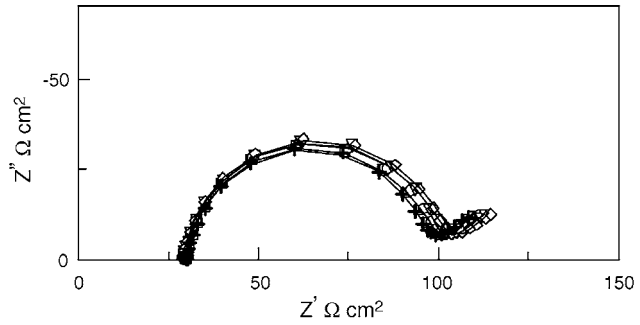

Fig. 4. Nyquist plot measured after hybridization reaction with ssDNA non complementary target, under various concentrations. 0 nmol ml^{-1} (+); 0.25 nmol ml^{-1} (□); 0.5 nmol ml^{-1} (◯); 0.75 nmol ml^{-1} (▽) and 1 nmol ml^{-1} (◊). Impedance spectra were acquired at −1400 mV vs. (SCE) in PBS electrolyte, pH 7. The symbols are the experimental data, and the solid lines are results from the fitting data.

excellent fit to the experimental data. This equivalent electrical circuit consists of resistive and capacitive elements:

- R_1 is the solution resistance.
- The constant phase element Q_1 is then related to the space charge capacitance at the PPy-DNA/electrolyte interface.
- R_2 is related to the charge transfer resistance at the polymer-DNA/electrolyte interface.
- The constant phase element Q_2 is the Warburg impedance due to mass transfer to the electrode surface.

The impedance of the constant phase element is defined as: $Z_Q = (j\omega)^{-n}/Y_0$, where Y_0 is the modulus, ω the angular phase and n the phase ($0 \leq n \leq 1$). The constant phase element reflects the non-homogeneity of the layer. Where Y_0 is a proportionality constant containing the diffusion coefficient and other parameters which depend on the characteristics of the electrochemical system, $j^2 = -1$, $\omega = 2\pi f$ is the angular frequency, and n is an exponent ($0 \leq n \leq 1$). In fact Q represents a very general dispersion relation. For $n = 1$, it models a capacitance with $C = Y_0$; for $n = 0$, a resistance with $R = Y_0^{-1}$. A special case is obtained for $n = 0.5$, that is, so called Warburg element [37]. This equivalent circuit gives a good description of the impedance data obtained ($\chi^2 \sim 10^{-4}$).

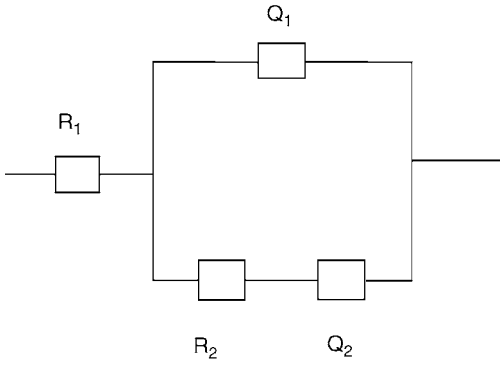

Scheme 3. Randles equivalent circuit model. The parameters of this circuit are listed in the text.

The calculated value of Q_1, R_2 and Q_2 are listed in Table 1. In the presence of ss-DNA complementary target the charge transfer resistance R_2 increases considerably. For Q_1, the value of n varies from 0.933 to 0.862 which shows that Q_1 can be considered as a capacitance C.

The faradaic impedance measurements were performed at −1.4 V versus SCE, at this potential the polypyrrole is in semi-conducting state and no electroactive specie is present. The measurement of electrical parameters of the polypyrrole-ssDNA and polypyrrole-dsDNA films allows to evidence the contribution of the conformational change of the polypyrrole after such steps and the influence of the negative charge on the polypyrrole.

These results show the decrease of the charge transfer resistance of the PPy-ssDNA film upon grafting of DNA probe and the increase of this charge transfer resistance upon hybridization reaction.

The change in the charge transfer resistance of the polypyrrole layers could be explained by the effect of the negative charge of ss-DNA and ds-DNA and of their conformational structures.

The decrease of charge transfer resistance in the case of the grafting of ss-DNA onto polypyrrole is explained on the basis of the negative charge of DNA. The polypyrrole could be considered as p-type semiconductor where the majority of the carriers are holes, as negatively charged ss-DNA molecules approaches the interface of polypyrrole its leads to increase of the majority carrier density and then a decrease of resistance of space charge region. The same behaviour was obtained in the case of interaction of DNA with p-type silicon semiconducor [38]. Moreover, the ss-DNA presents a random structure and the penetration of the flexible single DNA strand into the polymer pores increases the ionic concentration in the polypyrrole film.

The hybridization reaction between ss-DNA-polypyrrole and its complementary ss-DNA target will result in the helix formation and the increase of the length of the double strand

immobilized on the polypyrrole backbone. As single strands ss-DNA present a random coil structure, the double strands ds-DNA present a rigid helicoical chain. Thus, hybridization reaction induces significant change in the stiffness of the polypyrrole, leading to a decrease of intrinsic conjugation of the polypyrrole. This change of structural conformation of polypyrrole backbone should modify the related electrical parameters such as the resistance of electron transfer [29,33] the oxidation potential [30,33] and the conductivity [27].

On the contrary, an increase of the conductance of the conducting polymer film was observed in the case of the hybridization reaction based on the incorporated oligonucleotide into polypyrrole films formed on carbon nanotube modified electrode [28] or in the case of ODN-functionalized polyterthiophene [32] where measurements were performed in both case at open circuit voltage and then the polymers are in the conducting state and where electron transfer occurs.

The capacitance shows an increase after hybridization reaction which is due to the increase of the density of negative charges of phosphate groups upon hybridization as observed in [33] and [38].

3.3. Calibration curves from impedance measurements

The calibration curves corresponding to the respective variation of the capacitance C and the resistance R_2 of the PPy-DNA electrode after hybridisation reaction are presented in Figs. 5 and 6. Both these curves show large variations with concentrations of DNA target.

In the case of non-complementary target, no variation in these parameters was observed due to the absence of hybridization reaction between the DNA probe grafted on polypyrrole and the non-complementary DNA present in solution.

From Fig. 5, the capacitance decreases after addition of DNA target and presents a minimum value for the concentration of 0.05 nmol ml^{-1} of the complementary DNA target. The value then increases upon addition of DNA target.

The ss-DNA grafted on PPy in the absence of complementary ss-DNA target is in the folded configuration, where ss-DNA occupies a region of space smaller than its natural size because of inter-segment interactions resulting from steric or electrostatic repulsion [39]. When hybridization with a complementary sequence DNA target occurs, the folding configuration is converted into a rigid, linear double helix DNA (dsDNA), where the space occupied is much higher [40] and the densities of the charged phosphate group increase, in addition, the number of the condensed counter ions increases leading to an increase in capacitance. The variation of both parameters (configuration and charge density) compete and lead to a non monotoneous variation of capacitance in the range of concentration of complementary DNA target 0–2 nmol ml^{-1} and then the increase of charge density becomes predominant and capacitance increases as concentration increases. An increase of capacitance of the Ppy-DNA film was also observed in [33]. Piro et al. [41] showned an increase of capacitance of electroactive polymer upon hybridization reaction and attributed this variation to a surface reorganization of DNA and the increase of the density of the charge in the vicinity of the film.

A quantitative study of the sensitivity was made by analyzing the variation of charge transfer resistance R_2 with continuous addition of the ss-DNA complementary target from 0 to 5.5 nmol ml^{-1}. Fig. 6 shows the increase of R_2 with the amount of ODN target, which describes a linear variation with the DNA target concentration. The sensitivity of complementary ODN was calculated from the slope at the origin of this curve, and the value obtained was 21.6 Ω cm^{-2} μM^{-1}. Taking into account of a signal to noise ratio of 3, the detection limit using conventional method was determined as 1 pmol (0.2 nM) of ODN target. This value is lower of one order of magnitude than that obtained with the

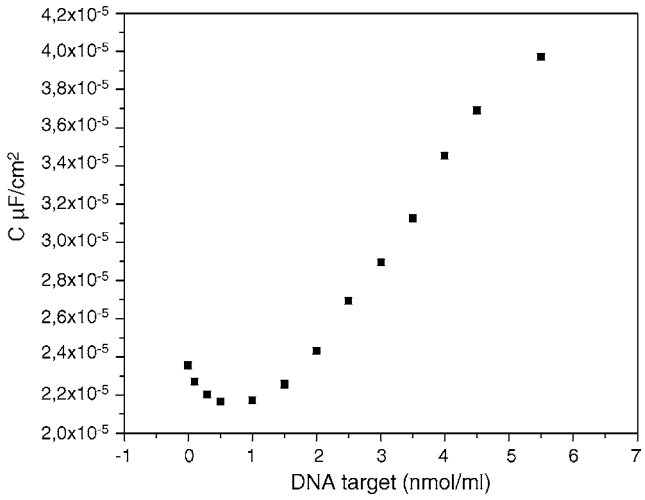

Fig. 5. Calibration plot showing the change in the capacitance $C = Q_1$ of the chip vs the complementary ss-DNA target concentration.

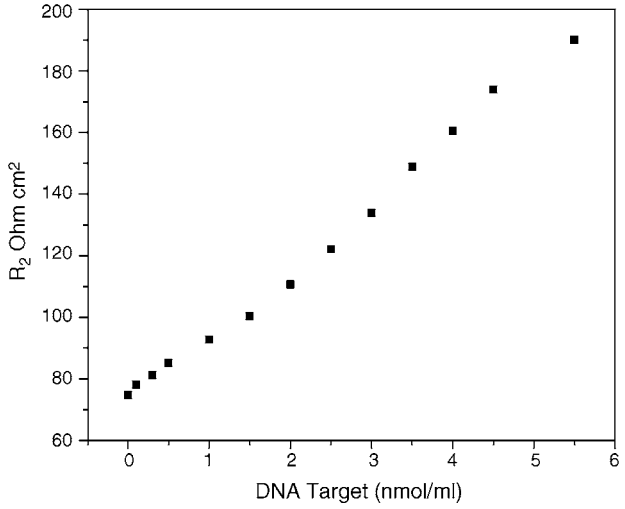

Fig. 6. Calibration plot showing the variation of the resistance R_2 versus the complementary target concentration.

same system, the DNA-functionalized polypyrrole electrode, measuring variation of oxidation current at constant potential of the polypyrrole, which was evaluated to 10 pmoles [11].

Comparing this detection limit to the value obtained by other systems, where 1 nmol was found with electrochemical response of polythiophene [42], 1 nmol, using the system with fluorescence probe [43], 10 nmol, with nanoparticle probes [44] and 20 pmol, with system using catalytic activity of enzyme [45], the value of 1 pmol, obtained with our system using DNA-functionnalized polypyrrole as interface and electrochemical impedance spectroscopy as direct electrical method of detection, appears very promising in the application in DNA chips.

4. Conclusion

The large surface area obtained by porous polypyrrole leads to increase in the density of immobilized DNA probes, which helps to monitor more easily the DNA hybridization reaction. In this study, we have demonstrated that by using electrochemical impedance spectroscopy combined with theoretical models involving the Randles circuit it is possible to determine modifications in the electrical properties of polypyrrole-DNA film upon the hybridization reaction. Using a calibration curve a good correlation between charge transfer resistance and the concentration of DNA target in solution in the range of 100 pmol ml^{-1} to 5.5 nmol ml^{-1} was demonstrated, which implies a detection limit of 1 pmol. A selectivity of detection is shown using this label-free detection technique which will then be applied to the detection of one mismatch and to the fabrication of an electrical biochip, without any PCR amplification step.

Acknowledgement

This work was financially supported by the EC Nanobiotechnology Project ELISHA.

References

[1] J. Hodgson, Nat. Biotechnol. 16 (1998) 725.
[2] H.C. Hoch, L.W. Jelinski, H.G. Craighead, Nanofabrications and Biosystems, Cambridge University Press, New York, 1996.
[3] M. Heller, J. Annu. Rev. Biomed. Eng. 4 (2002) 129.
[4] J. Van Ness, S. Kalbfleisch, C.R. Petri, M.W. Reed, J.C. Tabone, N.M.J. Vermeulen, Nucleic Acids Res. 19 (1991) 3345.
[5] W.P. Alexender, K.W. Lauren, M.G. Rosina, J. Am. Chem. Soc. 124 (2002) 14601.
[6] W.P. Alexender, K.W. Lauren, M.G. Rosina, Proc. Natl. Acad. Sci. U.S.A. 98 (2001) 3701.
[7] J.A. Ferguson, T. Boles, C. Adams, D. Walt, Nat. Biotech. 14 (1996) 1681.
[8] D. Memed, S. Reza, P. Erhan, Biosens. Bioelectron. 18 (2003) 1355.
[9] W. Jian, J.B. Allen, Anal. Chem. 73 (2001) 2207.
[10] A.T. Liz, K. Janusz, J. Mira, J. Jiri, J. Am. Chem. Soc. 125 (2003) 324.
[11] H. Korri-Youssoufi, A. Yassar, Biomacromolecules 2 (2001) 58.
[12] W. Joseph, Chem. Eur. J. 5 (1999) 1681.
[13] K. Kagan, K. Masaaki, T. Eiichi, Meas. Sci. Technol. 15 (2004) R1.
[14] E. Palecek, M. Fojta, Anal. Chem. 73 (2001) 74A.
[15] F. Patolsky, A. Lichtenstein, I. Willner, Nat. Biotechnol. 19 (2001) 253.
[16] L. Yi-Tao, L. Chen-Zhong, K. Heinz-Bernhard, S.L. Jeremy, Biophys. J. 84 (2003) 3218.
[17] B. Christin, S. Per, B. Jan, J. Gillis, Electroanalysis 11 (1999) 156.
[18] Z.L. Chen, Tao.L. Yi, S.L. Jeremy, B.K. Heinz, ChemComm (2004) 574.
[19] C.H. Tin, G.E. Anthony, Biosens. Bioelectron. 19 (11) (2004) 1537.
[20] Y. Zhang, M.Y. Coyne, S.G. Will, C.H. Levenson, E.S. Kawasaki, Nucleic Acids Res. 14 (1991) 3929.
[21] G.T. Harmanson, Bioconjugate Techniques, Academic Press, San Diego, 1995.
[22] Z. Junhui, C. Hong, Y. Ruifu, Biotechnol. Adv. 1 (1997) 43.
[23] Z. Yang, I. Engquist, M. Wride, J.M. Kauffmann, U. Gelius, B. Liedberg, Langmuir 13 (1997) 3210.
[24] E.S. Christine, R.S. Venkatram, P.V. Joseph, L. Robert, Proc. Natl. Acad. Sci. U.S.A. 94 (1997) 8948.
[25] T.A. Skotheim, Handbook of Conductive Polymers, Marcel Dekker, New York, 1986.
[26] D.S. Minehan, K.A. Marx, S.K. Tripathy, Macromolecules 27 (1994) 777.
[27] J. Wang, M. Jiang, A. Fortes, B. Mukherjee, Anal. Chim. Acta 402 (1999) 7.
[28] H. Cai., Y. Xu., P.-G. He, Y.-Z. Fang, Electroanalysis 15 (2003) 1864.
[29] A. Ramanviciene, A. Ramanavicius, Anal. Bioanal. Chem. 379 (2004) 287.
[30] H. Korri-Youssfi, F. Garnier, P. Srivastava, P. Godillot, A. Yassar, J. Am. Chem. Soc. 119 (1997) 7388.
[31] F. Garnier, H. Korri-Youssoufi, P. Srivastava, B. Mandrand, T. Delair, Synth. Met. 100 (1999) 89.
[32] T.Y. Lee, Y.-B. Shim, Anal. Chem. 73 (2001) 5629.
[33] H. Peng, C. Soeller, N. Vigar, P.A. Kilmartin, M.B. Cannell, G.A. Bowmaker, R.P. Cooney, J. Travas-Sejdic, Biosensens. Bioelectron. 20 (2005) 1821.
[34] P. Godillot, H. Korri-Youssoufi, F. Garnier, A. El Kassmi, P. Srivastava, Synth. Met. 83 (1996) 117.
[35] J.L. Brèdas, G.B. Street, Acc. Chem. Res. 18 (1985) 309–315.
[36] J.E.B. Randles, Discuss. Faraday Soc. 1 (1947) 11.
[37] B.A. Boukamp, Solid State Ionics 20 (1986) 31.
[38] W. Cai, J.R. Peck, D.W. van der Weide, R.J. Hamers, Biosens. Bioelectron. 19 (2004) 1013.
[39] S.B. Smith, Y. Cui, C. Bustamante, Science 271 (1996) 795.
[40] C.G. Baumann, S.B. Smith, V.A. Bloomfield, C. Bustamante, Proc. Natl. Acad. Sci. U.S.A. 94 (1997) 6185.
[41] B. Piro, J. Haccoun, M.C. Pham, L.D. Tran, A. Rubin, H. Perrot, C. Gabrielli, J. Electroanal. Chem. 577 (2005) 155.
[42] J. Cha, J.I. Han, Y. Choi, D.S. Yoon, K.W. Oh, G. Lim, Biosens. Bioelectron. 18 (2003) 1241.
[43] L.E. Morisson, L.M. Stols, Biochemistry 32 (1993) 3095.
[44] S.J. Park, T.A. Taton, C.A. Mirkin, Sciences 295 (2002) 1503.
[45] C.N. Campbell, D. Gal, N. Cristler, C. Banditrat, A. Heller, Anal. Chem. 74 (2002) 158.